Computer Assisted Methods in Engineering and Science, **24**: 181–198, 2017.

Flexural stability analysis of stiffened plates using the finite element method

Saleema Panda, Manoranjan Barik
Department of Civil Engineering
National Institute of Technology
Rourkela, Odisha 769008, India
e-mail: manoranjanbarik@yahoo.co.in

A four-noded stiffened plate element has been developed which has all the advantages and efficiency of an isoparametric element to model arbitrary shaped plates, but without the disadvantage of the shear-locking problem inherent in the isoparametric element. Another unique feature is that the arbitrary placement of the stiffener inside the plate element is without any restriction of its orientation. The boundary conditions have been incorporated in a general manner so as to accommodate the curved as well as the straight-edged boundaries. The element has been used for stability analysis of arbitrary shaped stiffened plates.

Keywords: arbitrary shape, finite element method, thin plate, stability analysis.

Novelty: In this work, a plate bending element is proposed, which can model any arbitrary shape as efficiently as an isoparametric element. As it does not include the shear deformation, thin plate problems can be considered without any numerical difficulties as observed in isoparametric elements. This element is generalized to accommodate any arbitrary shapes of the plate geometry. The mesh divisions for plates with irregular boundaries using the finite element method are sometimes difficult. However, this element eliminates such complexities as the mesh divisions are done in the mapped square plate. The stiffener is modeled so that it can be of any shape, dispositions and be arbitrarily placed on the plate.

1. Introduction

Stiffened plates of various geometrical configurations are one of the important structural elements in many engineering applications. The buckling analysis of such structures becomes inevitable as they are frequently subjected to inplane-loads. The static and dynamic studies of stiffened plates abound in literature, however stability analyses of stiffened plates of arbitrary forms are rare.

Mizusawa et al. [12] were the first to analyze skew stiffined plates for buckling using the Rayleigh-Ritz method with B-spline as the coordinate functions. They studied the effect of various stiffness parameters of the stiffener on the buckling load. Brown and Yettram [7] proposed a conjugate load/displacement method of analysis for the determination of the elastic buckling loads of stiffened plates under various loading and support conditions. They highlighted the significance of the torsional rigidity of the stiffeners to the overall behavior of the complete structure. This method demands the placement of the stiffeners to be oriented parallel to the x or y-coordinate axes. They analyzed only rectangular stiffened plates for buckling. Shen et al. [19] presented a semi-analytical approach using the Rayleigh-Ritz method with B-spline as coordinate functions to analyze the stability behavior of rectangular stiffened plates. The finite element method was first employed by Mukhopadhyay and Mukherjee [14] for skew stiffened plate buckling. They presented buckling results for square and skew stiffened plates and studied the effect of stiffener rigidity, torsional stiffness and eccentricity of the stiffener on the buckling load. Although an isoparametric quadratic plate bending element as used in their formulation can accommodate irregular plate shapes, they did not present any results for plates having curved boundaries. An extensive review on the stability

of stiffened plates was carried out by Bedair [6], and he also presented a numerical method for the prediction of the buckling load of multi-stiffened plates under uniform compression following the philosophy of plate idealization. In his analysis he employed the sequential quadratic programming to the strain energy components of the plate and the stiffener elements in terms of the out-of-plane and in-plane displacement functions. He also presented a number of examples pertaining to the straight-edged orthogonally stiffened plates. However, this method lacks the ability to analyze the curved boundary stiffened plates buckling.

Rikards et al. [21] presented a buckling analysis of stiffened plates and shells using a triangular finite element based on the first-order shear deformation theory. Buckling analysis of laminated stiffened plates using a layerwise (zigzag) finite element formulation was discussed by Guo et al. [10]. The plate and stiffeners were modeled using degenerated shell and 3D beam elements respectively. Srivastava et al. [24] used a nine-noded isoparametric quadratic element to investigate buckling loads of stiffened plates under different aspect ratios, boundary conditions and partial edge loadings. Peng et al. [17, 18] studied the buckling analysis of rectangular stiffened plates which are studied by using the element-free and meshless Galerkin method with the first-order shear deformation theory. Mittelstedt [11] analyzed stiffened orthotropic composite plates using a closed form analytical method. A meshfree method was used by Tamijani and Kapania [26] for buckling analysis of curved stiffened plates. They employed the first-order shear deformation theory to model the finite elements and applied the penalty method to satisfy the boundary conditions. Fenner and Watson [9] studied the buckling response of stiffened plates due to variation in the cross-sectional geometry of the line junctions between the component plates that form the cross section of the stiffened panel. Singh and Chakrabarti [23] discussed the buckling analysis of laminated composites based on the higher order zig-zag theory using a nine-noded C0 continuous isoparametric finite element. Ramkumar and Kang [20] investigated the buckling analysis of thin-walled box type structures using finite element software ANSYS. Coburn et al. [8] presented an analytical method using the Rayleigh Ritz approach for analysis of stiffened variable angle tow panels. Shi et al. [22] used the first deformation theory by to model both plate and beam element for analysis of curved stiffened plates. Patel and Sheikh [16] studied the buckling behavior of laminated composite stiffened plate under partial edge loading. They used eight-noded isoparametric shell element and three-noded curved beam element to model plate and stiffeners respectively.

A new four-noded bare plate bending element for the free vibration and buckling analysis of arbitrary shaped plates has already been presented by the authors in [4, 15]. The same element was modified to include the inplane-displacements so as to enable the stiffened plate analysis. It was successfully employed by the authors for the free vibration analysis of stiffened plates [3]. In this paper, the same stiffened plate bending element was used to extend the work for analyzing the buckling of the arbitrary stiffened plates. The isoparametric element based on the Mindlin plate theory suffers shear locking and spurious mechanism when used for thin plates. The present formulation is based on the Kirchoff thin plate theory and is thus free from such disadvantages. Use of this element buckling analysis of the circular stiffened plates was carried out for the first time. The efficiency of the element is shown by comparing the buckling results of various stiffened plates configurations with those presented by others.

2. Proposed analysis

2.1. Coordinate transformation

The arbitrary shape of the whole plate is mapped onto a master plate of square region $[-1, +1]$ in the $s-t$ plane (Fig. 1) with the help of the relation [28] given by:

$$x = \sum_{i=1}^{12} N_i(s,t)\, x_i, \qquad y = \sum_{i=1}^{12} N_i(s,t)\, y_i, \tag{1}$$

where (x_i, y_i) are the coordinates of the i-th node on the boundary of the plate in the $x-y$ plane and $N_i(s,t)$ are the corresponding cubic serendipity shape functions. The master plate in the $s-t$ plane, which is square instead of arbitrary, is divided into a number of rectangular elements. For each rectangular element in the $s-t$ plane, twelve number of suitable nodes of its periphery are chosen and their (x,y) coordinates are determined by using Eq. (1), which is based on the mapping of the whole arbitrary plate to the master plate (Fig. 1). Then with the (x,y) coordinates of the twelve nodes on the boundary of each rectangular element being known, each element is mapped to a master element of square region $[-1,+1]$ in the $\xi-\eta$ plane as shown in Fig. 2 in a similar way as the original plate is mapped onto the master plate in the $s-t$ plane using the same cubic serendipity functions given in Eq. (1), but now the variables changed from (s,t) to $(\xi-\eta)$.

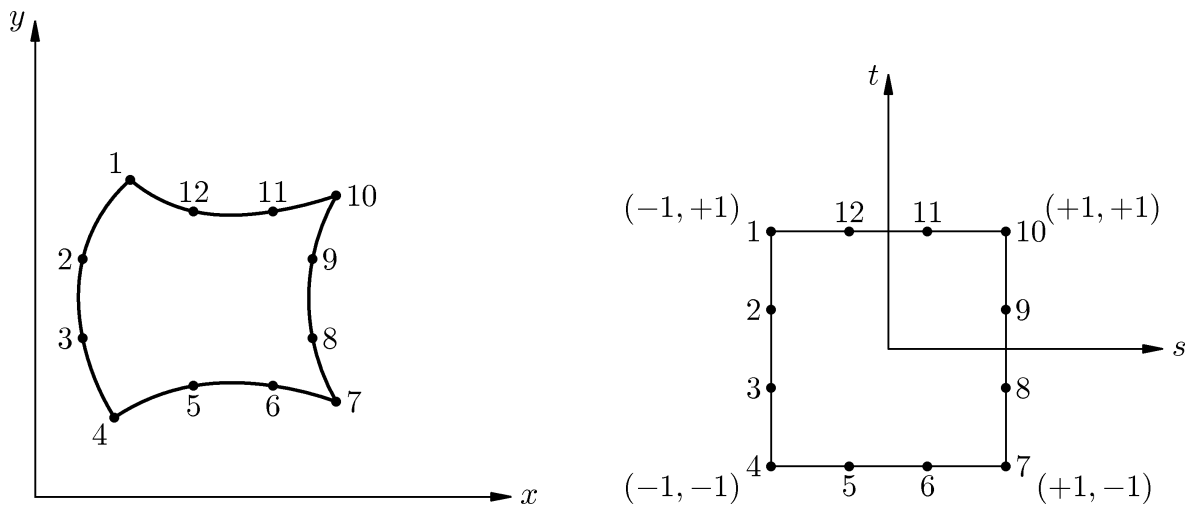

Fig. 1. Mapping of original arbitrarily shaped plate to master plate.

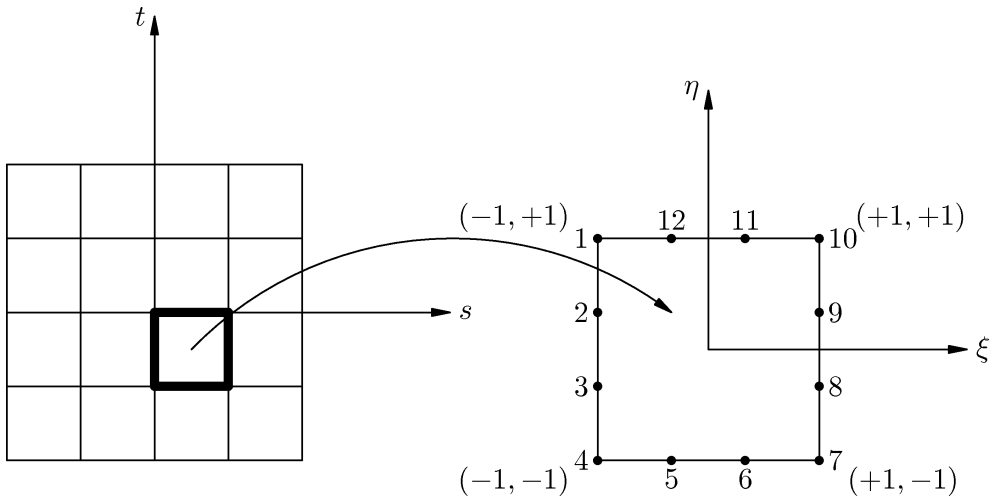

Fig. 2. Mapping of the element from $s-t$ to $\xi-\eta$ plane.

2.2. Displacement function

As the element is in the $\xi-\eta$ plane, the shape functions as well as the nodal parameters for the displacements and slopes are expressed in terms of the coordinates ξ and η instead of the x and y

coordinates of the parent ACM (Adini and Clough [1], Melosh [2]) element. Thus, the displacement field can be written as

$$\{f\} = \begin{Bmatrix} u \\ v \\ w \end{Bmatrix} = \begin{Bmatrix} [N_u] \\ [N_v] \\ [N_w] \end{Bmatrix} \{\delta_p\}, \tag{2}$$

$$[N_u] = [N_u^1 \ 0 \ 0 \ 0 \ 0 \ N_u^2 \ 0 \ 0 \ 0 \ 0 \ N_u^3 \ 0 \ 0 \ 0 \ 0 \ N_u^4 \ 0 \ 0 \ 0 \ 0], \tag{3}$$

$$[N_v] = [0 \ N_v^1 \ 0 \ 0 \ 0 \ 0 \ N_v^2 \ 0 \ 0 \ 0 \ 0 \ N_v^3 \ 0 \ 0 \ 0 \ 0 \ N_v^4 \ 0 \ 0 \ 0], \tag{4}$$

$$[N_w] = [0 \ 0 \ N_w^1 \ N_{\theta_\xi}^1 \ N_{\theta_\eta}^1 \ 0 \ 0 \ N_w^2 N_{\theta_\xi}^2 \ N_{\theta_\eta}^2 \ 0 \ 0 \ N_w^3 \ N_{\theta_\xi}^3 \ N_{\theta_\eta}^3 \ 0 \ 0 \ N_w^4 \ N_{\theta_\xi}^4 \ N_{\theta_\eta}^4], \tag{5}$$

$$\{\delta_p\} = \left[u_1 \quad v_1 \quad w_1 \quad \left(\frac{\partial w}{\partial \xi}\right)_1 \quad \left(\frac{\partial w}{\partial \eta}\right)_1 \ldots\ldots \quad u_4 \quad v_4 \quad w_4 \quad \left(\frac{\partial w}{\partial \xi}\right)_4 \quad \left(\frac{\partial w}{\partial \eta}\right)_4 \right]^T. \tag{6}$$

The shape functions for the displacement fields corresponding to a particular node, say the jth node can be expressed [28] as

- for the inplane-displacements:

$$N_u^j = N_v^j = \frac{1}{4}(1+\xi_0)(1+\eta_0), \tag{7}$$

- and for the out of plane displacements:

$$[N_w^j, \ N_{\theta_\xi}^j, \ N_{\theta_\eta}^j] = \frac{1}{8}\left[(\xi_0+1)(\eta_0+1)\left(2+\xi_0+\eta_0-\xi^2-\eta^2\right), \ \xi_j(\xi_0+1)^2(\xi_0-1)(\eta_0+1), \right.$$
$$\left. \eta_j(\xi_0+1)(\eta_0+1)^2(\eta_0-1)\right], \tag{8}$$

where $\xi_0 = \xi\xi_j$, $\eta_0 = \eta\eta_j$.

2.3. Stiffness matrix of the plate element

The stress-strain relation of the plate element is obtained as

$$\{\sigma\} = [D]\{\varepsilon\} = \begin{Bmatrix} [D]_a & \\ & [D]_f \end{Bmatrix} \{\varepsilon\}, \tag{9}$$

where

$$\{\sigma\} = \left\{F_x \quad F_y \quad F_{xy} \quad M_x \quad M_y \quad M_{xy}\right\}^T. \tag{10}$$

When isotropic material is considered:

$$[D]_a = \frac{Eh}{1-\nu^2}\begin{Bmatrix} 1 & \nu & 0 \\ \nu & 1 & 0 \\ 0 & 0 & \dfrac{1-\nu}{2} \end{Bmatrix} \tag{11}$$

and

$$[D]_f = \frac{h^2}{12}[D]_a. \tag{12}$$

The generalized strains are given by

$$\{\varepsilon\} = \left\{ \frac{\partial u}{\partial x} \quad \frac{\partial v}{\partial y} \quad \left(\frac{\partial u}{\partial y} + \frac{\partial v}{\partial x}\right) \quad -\frac{\partial^2 w}{\partial x^2} \quad -\frac{\partial^2 w}{\partial y^2} \quad 2\frac{\partial^2 w}{\partial x \partial y} \right\}^T. \tag{13}$$

By using the interpolation functions of u, v and w given in Eq. (2) and making use of the relationships of the first and second order derivatives between the (x, y) and (ξ, η) coordinate systems [5], the strain can be expressed in terms of nodal displacements as

$$\{\varepsilon\} = [B]\delta. \tag{14}$$

The stiffness matrix of the plate element is given by

$$[K]_e = \iint [B]^T [D] [B] |J| \, d\xi \, d\eta, \tag{15}$$

where

$$[J] = \begin{Bmatrix} \dfrac{\partial x}{\partial \xi} & \dfrac{\partial y}{\partial \xi} \\ \dfrac{\partial x}{\partial \eta} & \dfrac{\partial y}{\partial \eta} \end{Bmatrix}. \tag{16}$$

2.4. Stiffness matrix of the stiffener element

The stiffener is modeled as a separate element and the formulation of its stiffness matrix is carried out by considering the axial force, bending moment and torsional moment. As a general case, a curved stiffener having eccentricity with respect to the mid-plane of the plate and placed anywhere within the plate element is considered. Since the stiffener is curved, its axis direction changes from point to point, hence a local (x', y') axis is considered along the tangent to the stiffener at the Gaussian integration point making an angle α with the global (x, y) axis as shown in Fig. 3. The generalized stress-strain relationship of an eccentric stiffener in the local (x', y') axis at the Gauss point can be expressed as

$$\{\sigma_s\} = [D_s]\{\varepsilon_s\}, \tag{17}$$

where

$$\{\sigma_s\} = \begin{Bmatrix} F_s & M_s & T_s \end{Bmatrix}^T, \tag{18}$$

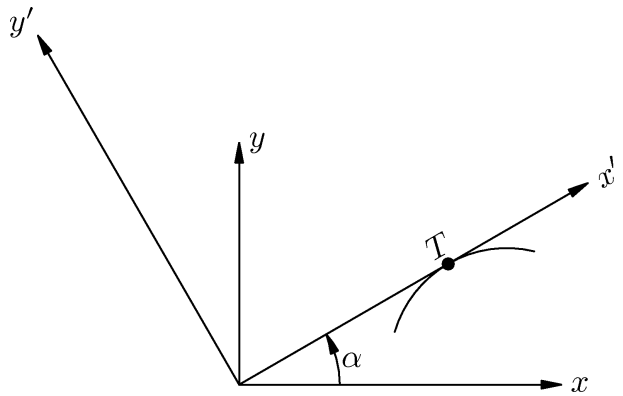

Fig. 3. Coordinate axes at any point of a curved stiffener.

$$\{\varepsilon_s\} = \left\{ \frac{\partial u'}{\partial x'} \quad -\frac{\partial^2 w'}{\partial x'^2} \quad -\frac{\partial^2 w'}{\partial x'\,\partial y'} \right\}^T, \tag{19}$$

$$[D_s] = \begin{bmatrix} EA_s & ES_s & 0 \\ ES_s & EI_s & 0 \\ 0 & 0 & GJ_s \end{bmatrix}. \tag{20}$$

Expressing Eq. (19) in global (x, y) axis system,

$$[\varepsilon_s] = [T_s]\{\overline{\varepsilon_s}\}, \tag{21}$$

where

$$[T_s] = \begin{bmatrix} \cos^2\alpha & \sin^2\alpha & \frac{1}{2}\sin 2\alpha & 0 & 0 & 0 \\ 0 & 0 & 0 & \cos^2\alpha & \sin^2\alpha & -\frac{1}{2}\sin 2\alpha \\ 0 & 0 & 0 & -\frac{1}{2}\sin 2\alpha & \frac{1}{2}\sin 2\alpha & -\frac{1}{2}\cos 2\alpha \end{bmatrix}, \tag{22}$$

$$\{\varepsilon_s\} = \left\{ \frac{\partial u}{\partial x} \quad \frac{\partial v}{\partial y} \quad \left(\frac{\partial u}{\partial y} + \frac{\partial v}{\partial x}\right) \quad -\frac{\partial^2 w}{\partial x^2} \quad -\frac{\partial^2 w}{\partial y^2} \quad 2\frac{\partial^2 w}{\partial x\,\partial y} \right\}^T. \tag{23}$$

As the strain vector is expressed in terms of displacements at the mid-plane of the plate, the displacement shape function used is the same as that of the plate element, which yields the stiffness matrix of the stiffener in terms of the nodal parameters of the plate element. By this process, the compatibility between the plate and the stiffener element is retained and any additional incorporation of degrees of freedom for the stiffener element is avoided. Hence, using the interpolation functions of Eq. (7) and (8), Eq. (23) can be written as

$$\{\overline{\varepsilon_s}\} = \{\varepsilon\} = [B]\{\delta\}. \tag{24}$$

Hence,

$$\{\varepsilon_s\} = [T_s][B]\{\delta\} = [B_s]\{\delta\}. \tag{25}$$

The stiffness of the stiffener element is expressed in terms of nodal degrees of freedom of that of the plate element and thus contributes to the stiffness of the actual plate element. The stiffness matrix of the stiffener element can be expressed as

$$[K_s]_e = \int [B_s]^T [D_s][B_s]dl = \int [B_s]^T [D_s][B_s]|J_{st}|\,d\lambda, \tag{26}$$

where l is taken along the stiffener axis in $x-y$ plane and λ is in the direction of the stiffener axis in the $\xi-\eta$ plane and the Jacobian $|J_{st}|$ is given by

$$|J_{st}| = \frac{dl}{d\lambda}, \tag{27}$$

which is calculated by the ratio of the actual length to the length on the mapped domain considering any segment of the stiffener.

2.5. Geometric stiffness matrix of the plate element

Buckling or the loss of stability when the load reaches a certain critical value, is caused by geometrically nonlinear effects. The geometric stiffness arises from a coupling between the linear elastic stresses and the nonlinear terms in the strain-displacement relations. So, for the analysis of the buckling behavior, the action of the in-plane loads causing bending strains is considered, by which the stiffness matrix is modified by another matrix known as the geometric stiffness matrix.

The expression for the strain at the mid-plane of the plate can be written as

$$\{\varepsilon\} = \{\varepsilon_{pE}\} + \{\varepsilon_{pG}\}, \tag{28}$$

where $\{\varepsilon_{pE}\}$ and $\{\varepsilon_{pG}\}$ are the elastic and the geometric plate strain [23] respectively, and are given by

$$\{\varepsilon_{pE}\} = \begin{Bmatrix} \dfrac{\partial u}{\partial x} \\ \dfrac{\partial v}{\partial y} \\ \dfrac{\partial u}{\partial y} + \dfrac{\partial v}{\partial x} \\ \dfrac{\partial w}{\partial x} \\ \dfrac{\partial w}{\partial y} \end{Bmatrix} \tag{29}$$

and

$$\{\varepsilon_{pG}\} = \begin{Bmatrix} \dfrac{1}{2}\dfrac{\partial w}{\partial x}^2 + \dfrac{1}{2}\dfrac{\partial u}{\partial x}^2 + \dfrac{1}{2}\dfrac{\partial v}{\partial x}^2 \\ \dfrac{1}{2}\dfrac{\partial w}{\partial y}^2 + \dfrac{1}{2}\dfrac{\partial u}{\partial y}^2 + \dfrac{1}{2}\dfrac{\partial v}{\partial y}^2 \\ \dfrac{\partial w}{\partial x}\dfrac{\partial w}{\partial y} + \dfrac{\partial u}{\partial x}\dfrac{\partial u}{\partial y} + \dfrac{\partial v}{\partial x}\dfrac{\partial v}{\partial y} \\ 0 \\ 0 \end{Bmatrix}. \tag{30}$$

The geometric stiffness matrix [14, 25] of the plate element can be obtained as

$$[K_{pG}]_e = \iint [B_{pG}]^T [\overline{\sigma}][B_{pG}]dx\,dy = \iint [B_{pG}]^T [\overline{\sigma}][B_{pG}]|J|d\xi\,d\eta, \tag{31}$$

$$[\overline{\sigma}] = \int_{-h/2}^{h/2} [H_{pG}]^T [\sigma_p][H_{pG}]dz, \tag{32}$$

$$[B_{pG}] = [T_{pG}][\overline{B}_{pG}], \tag{33}$$

$$[\overline{B}_{pG}] = \left[\left(\frac{\partial N_w}{\partial \xi}\right) \quad \left(\frac{\partial N_w}{\partial \eta}\right) \quad \left(\frac{\partial^2 N_w}{\partial \xi^2}\right) \quad \left(\frac{\partial^2 N_w}{\partial \eta^2}\right) \quad \left(\frac{\partial^2 N_w}{\partial \xi \eta}\right)\right]^T, \tag{34}$$

$$[\overline{T}_{pG}] = \begin{bmatrix} [T_{F3}] & 0 \\ [T_{F1}] & [T_{F2}] \end{bmatrix}, \tag{35}$$

$$[\overline{T}_{F1}] = -[J2]^{-1}[J1][J]^{-1}, \tag{36}$$

$$[\overline{T}_{F2}] = -[J2]^{-1}, \tag{37}$$

$$[\overline{T}_{F3}] = [J]^{-1}, \tag{38}$$

$$[J1] = \begin{bmatrix} \dfrac{\partial^2 x}{\partial \xi^2} & \dfrac{\partial^2 y}{\partial \xi^2} \\ \dfrac{\partial^2 x}{\partial \eta^2} & \dfrac{\partial^2 y}{\partial \eta^2} \\ \dfrac{\partial^2 x}{\partial \xi \eta} & \dfrac{\partial^2 y}{\partial \xi \eta} \end{bmatrix}, \tag{39}$$

$$[J2] = \begin{bmatrix} -\left(\dfrac{\partial x}{\partial \xi}\right)^2 & -\left(\dfrac{\partial y}{\partial \xi}\right)^2 & \dfrac{\partial x}{\partial \xi}\dfrac{\partial y}{\partial \xi} \\ -\left(\dfrac{\partial x}{\partial \eta}\right)^2 & -\left(\dfrac{\partial y}{\partial \eta}\right)^2 & \dfrac{\partial x}{\partial \eta}\dfrac{\partial y}{\partial \eta} \\ -\left(\dfrac{\partial x}{\partial \xi}\dfrac{\partial x}{\partial \eta}\right) & -\left(\dfrac{\partial y}{\partial \xi}\dfrac{\partial y}{\partial \eta}\right) & \dfrac{1}{2}\left(\dfrac{\partial x}{\partial \xi}\dfrac{\partial y}{\partial \eta} + \dfrac{\partial x}{\partial \eta}\dfrac{\partial y}{\partial \xi}\right) \end{bmatrix}. \tag{40}$$

The matrix $[T_{pG}]$ is the transformation matrix which relates the strain vector in the $x-y$ coordinate to that in the $\xi-\eta$ coordinate system [5] as

$$\{\overline{\varepsilon}_{pG}(x,y)\} = [T_{pG}]\{\overline{\varepsilon}_{pG}(\xi,\eta)\}, \tag{41}$$

where

$$\{\overline{\varepsilon}_{pG}(x,y)\} = \left[\frac{\partial w}{\partial x} \quad \frac{\partial w}{\partial y} \quad -\frac{\partial^2 w}{\partial x^2} \quad -\frac{\partial^2 w}{\partial y^2} \quad 2\frac{\partial^2 w}{\partial x\,\partial y}\right]^T, \tag{42}$$

$$\{\overline{\varepsilon}_{pG}(\xi,\eta)\} = \left[\frac{\partial w}{\partial \xi} \quad \frac{\partial w}{\partial \eta} \quad -\frac{\partial^2 w}{\partial \xi^2} \quad -\frac{\partial^2 w}{\partial \eta^2} \quad 2\frac{\partial^2 w}{\partial \xi\,\partial \eta}\right]^T. \tag{43}$$

The stress matrix for the plate element is given by

$$[\sigma_p] = \begin{bmatrix} \sigma_x & \tau_{xy} & 0 & 0 & 0 \\ \tau_{xy} & \sigma_y & 0 & 0 & 0 \\ 0 & 0 & \sigma_x & 0 & \tau_{xy} \\ 0 & 0 & 0 & \sigma_y & \tau_{xy} \\ 0 & 0 & \tau_{xy} & \tau_{xy} & (\sigma_x + \sigma_y) \end{bmatrix}, \tag{44}$$

$$[H_{pG}] = \begin{bmatrix} 1 & 0 & 0 & 0 & 0 \\ 0 & 1 & 0 & 0 & 0 \\ 0 & 0 & z & 0 & 0 \\ 0 & 0 & 0 & z & 0 \\ 0 & 0 & 0 & 0 & -\frac{1}{2}z \end{bmatrix}. \tag{45}$$

2.6. Geometric stiffness matrix of the stiffener element

The geometric stiffness matrix of the stiffener element can be expressed as

$$[K_{sG}]_e = \iint [B_{sG}]^T [\overline{\sigma}][B_{sG}] dx\, dy = \iint [B_{sG}]^T [\overline{\sigma}][B_{sG}] |J_{st}| d\xi\, d\eta, \tag{46}$$

where

$$[B_{sG}] = [T_{sG1}][T_{pG}][\overline{B}_{pG}], \tag{47}$$

$$[\sigma_s] = \begin{bmatrix} \sigma_x A_s & 0 \\ 0 & \sigma_x I_s \end{bmatrix}, \tag{48}$$

$$[T_{sG1}] = \begin{bmatrix} \cos\alpha & \sin\alpha & 0 & 0 & 0 \\ 0 & 0 & -\cos^2\alpha & -\sin^2\alpha & \sin\alpha\cos\alpha \end{bmatrix}. \tag{49}$$

2.7. Boundary conditions for the stiffened plate

As a general case, the stiffness matrix for a curved boundary supported by elastic springs continuously spread in the directions of possible displacements and rotations along the boundary line is formulated, from which the specific boundary conditions can be obtained by incorporating the appropriate value of the spring constants. Considering a local axis system $x_1 - y_1$ at a point P on a curved boundary along the direction normal to the boundary at that point as shown in the Fig. 4, the displacement components along it can be found. Let the angle made by the local axis $x_1 - y_1$ with the global axis $x - y$ be β. Hence, the relationship between the two axes can be established as given below

$$\begin{Bmatrix} x \\ y \end{Bmatrix} = \begin{bmatrix} \cos\beta & -\sin\beta \\ \sin\beta & \cos\beta \end{bmatrix} \begin{Bmatrix} x_1 \\ y_1 \end{Bmatrix}. \tag{50}$$

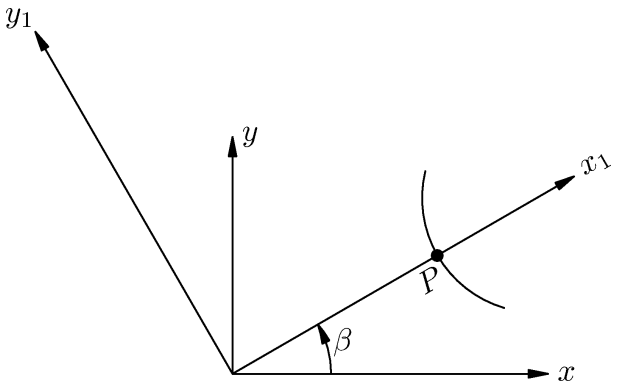

Fig. 4. Co-ordinate axes at any point of an elastically restrained curved boundary.

The relationship between the in-plane displacements in the local and the global coordinates at point p is given by

$$\begin{Bmatrix} u_1 \\ v_1 \end{Bmatrix} = \begin{bmatrix} \cos\beta & \sin\beta \\ -\sin\beta & \cos\beta \end{bmatrix} \begin{Bmatrix} u \\ v \end{Bmatrix}, \tag{51}$$

where u_1 and v_1 are the displacements along the direction of x_1 and y_1 respectively. The displacements at P which may be restrained can be expressed as

$$\{f_{bp}\} = \begin{Bmatrix} u_1 \\ v_1 \\ w \\ \theta_n \\ \theta_t \end{Bmatrix} = \begin{Bmatrix} u_1 \\ v_1 \\ w \\ \dfrac{\partial w}{\partial x_1} \\ \dfrac{\partial w}{\partial y_1} \end{Bmatrix}, \tag{52}$$

where θ_n and θ_t represent the slopes which are normal and transverse to the boundaries respectively. Substituting from Eqs. (50) and (51), Eq. (52) can be written as

$$\{f_{bp}\} = \begin{bmatrix} \cos\beta & \sin\beta & 0 & 0 & 0 \\ -\sin\beta & \cos\beta & 0 & 0 & 0 \\ 0 & 0 & 1 & 0 & 0 \\ 0 & 0 & 0 & \cos\beta & \sin\beta \\ 0 & 0 & 0 & -\sin\beta & \cos\beta \end{bmatrix} \begin{Bmatrix} u \\ v \\ w \\ \dfrac{\partial w}{\partial x} \\ \dfrac{\partial w}{\partial y} \end{Bmatrix}. \tag{53}$$

Expressing Eq. (53) in terms of the shape functions:

$$\{f_{bp}\} = [N_{bp}]\{\delta_p\}, \tag{54}$$

where

$$[N_{bp}] = \begin{bmatrix} \cos\beta & \sin\beta & 0 & 0 & 0 \\ -\sin\beta & \cos\beta & 0 & 0 & 0 \\ 0 & 0 & 1 & 0 & 0 \\ 0 & 0 & 0 & \cos\beta & \sin\beta \\ 0 & 0 & 0 & -\sin\beta & \cos\beta \end{bmatrix} \begin{Bmatrix} [N_u] \\ [N_v] \\ [N_w] \\ \dfrac{\partial [N_w]}{\partial x} \\ \dfrac{\partial [N_w]}{\partial y} \end{Bmatrix}. \tag{55}$$

The reaction components per unit length along the boundary line due to the spring constants corresponding to the possible boundary displacements given in Eq. (52) can be expressed as

$$\{f_{kp}\} = \begin{Bmatrix} f_{ku} \\ f_{kv} \\ f_{kw} \\ f_{k\alpha} \\ f_{k\beta} \end{Bmatrix} = \begin{Bmatrix} k_u u_1 \\ k_v v_1 \\ k_w w \\ k_\alpha \theta_n \\ k_\beta \theta_t \end{Bmatrix}, \tag{56}$$

where k_u, k_v ,k_w, k_α and k_β are the spring constants or restraints coefficients corresponding to the direction of u_1, v_1, w, θ_n and θ_t respectively

$$\{f_{kp}\} = [N_{kp}]\{\delta_p\}, \tag{57}$$

where

$$[N_{kp}] = \begin{bmatrix} k_u \cos\beta & k_u \sin\beta & 0 & 0 & 0 \\ -k_v \sin\beta & k_v \cos\beta & 0 & 0 & 0 \\ 0 & 0 & k_w & 0 & 0 \\ 0 & 0 & 0 & k_\alpha \cos\beta & k_\alpha \sin\beta \\ 0 & 0 & 0 & -k_\beta \sin\beta & k_\beta \cos\beta \end{bmatrix} \begin{Bmatrix} [N_u] \\ [N_v] \\ [N_w] \\ \dfrac{\partial [N_w]}{\partial x} \\ \dfrac{\partial [N_w]}{\partial y} \end{Bmatrix}. \tag{58}$$

Following the procedure similar to the case of the bare plate [4] the stiffness of the boundary for the stiffened plate can be expressed as

$$[K_{bp}] = \int [N_{bp}]^T [N_{kp}] |J_b| \, d\lambda_1, \tag{59}$$

where λ_1 is the direction of the boundary line in the $\xi - \eta$ plane and Jacobian $J_b = ds_1/d\lambda_1$. The Jacobian is the ratio of the actual length to the length of the mapped domain at any segment of the boundary length. The boundary stiffness is added to the global stiffness matrix.

3. Numerical examples

Stability analysis for the stiffened plates with various configurations and boundary conditions is carried out and the buckling parameters are tabulated and compared with the published results of other investigators wherever possible. The results are presented in tabular form which are obtained with a mesh division of 16×16 for the whole plate unless otherwise mentioned. The boundary conditions are indicated in the tables by means of letters C and S, denoting clamped and simply supported edges respectively, which start from the left edge of the plate and proceeds in a counter clockwise direction. Thus, CSCS denotes the boundary conditions having the left and right edge clamped and the other opposite edges simply supported. The plate element is shown by the solid line, while stiffener element is shown as dashed line.

3.1. Buckling of square stiffened plates

A number of square stiffened plates, shown in Fig. 5, with a concentric central stiffener, were analyzed for various stiffener sizes and flexural rigidities, and the buckling parameters are presented

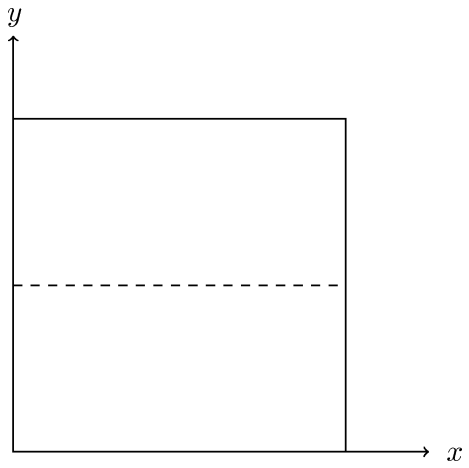

Fig. 5. Square stiffened plate.

in Table 1 for plates with different boundary conditions. The ratio of the cross-sectional area of the stiffener to that of the plate (A_s/bt) varied from 0.05 to 0.20 and the ratio of the bending stiffness of the stiffener to that of the plate (EI_s/bD) varied from 5 to 25. The torsional inertia of the stiffener was neglected in the analysis. The results are compared with the semi-analytic finite difference results [13] and the agreement is satisfactory enough. It is observed, that under uniaxial compression, with an increase in the ratio of bending stiffness or area ratio, the buckling parameter is constant for the clamped boundary and there is slight increase in the mixed boundary condition.

Table 1. Buckling parameter $k = \lambda b^2/\pi^2 D$ for square plate with a central concentric stiffener subjected to uniaxial and uniform compression in the stiffener direction ($\nu = 0.3$).

EI_s/bD	(A_s/bt)	Boundary condition			
		CCCC		CSSC	
		Present	[13]	Present	[13]
5	0.05	24.25	25.46	17.35	17.32
	0.10	24.25	25.46	17.15	17.05
	0.20	24.25	25.46	16.41	16.27
10	0.05	24.25	–	17.94	–
	0.10	24.25	–	17.93	–
	0.20	24.25	–	17.90	–
15	0.05	24.25	25.46	18.03	18.36
	0.10	24.25	25.46	18.03	18.36
	0.20	24.25	25.46	18.02	18.34
20	0.05	24.25	25.46	18.070	–
	0.10	24.25	25.46	18.068	–
	0.20	24.25	25.46	18.064	–
25	0.05	24.25	–	18.09	18.46
	0.10	24.25	–	18.09	18.46
	0.20	24.25	–	18.09	18.46

3.2. Buckling of simply supported rectangular stiffened plates

A series of simply supported rectangular stiffened plates with a concentric central stiffener, shown in Fig. 6, were analyzed for various proportions of the plate and of the stiffener and the buckling parameters are presented along with those of other investigators in Table 2. The ratio of the cross-sectional area of the stiffener to that of the plate (A_s/bt) varied from 0.05 to 0.20, and the ratio of the bending stiffness of the stiffener to that of the plate (EI_s/bD) varied from 5 to 20. The torsional inertia of the stiffener was neglected in the analysis. To analyze this problem, Mukhopadhyay [13] used the semi-analytic finite difference method whereas Mukhopadhyay and Abhijit [14] used the finite element method. Good agreement of the results was obtained when compared with the results of Timoshenko and Gere [27] and those of others. The buckling parameter $k = \lambda b^2/\pi^2 D$ for uniformly compressed all edges simply supported the square stiffened plate with varying stiffness

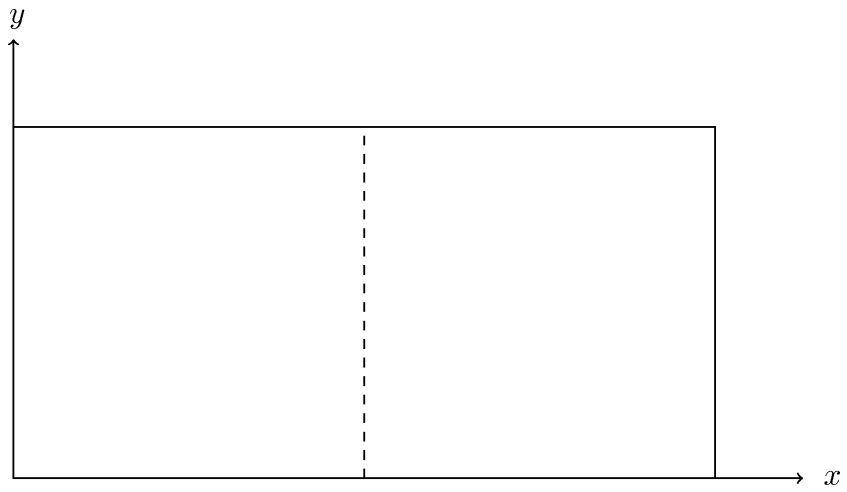

Fig. 6. Rectangular stiffened plate.

Table 2. Buckling parameter $k = \lambda b^2/\pi^2 D$ for uniformly compressed all edges simply supported rectangular stiffened plates ($\nu = 0.3$).

EI_s/bD	(A_s/bt)	Aspect Ratio (a/b)					
		1			2		
		Present	[27]	[14]	Present	[27]	[13]
5	0.05	11.84	12.0	11.72	7.93	7.96	7.93
	0.10	11.02	11.1	10.93	7.27	7.29	7.28
	0.20	9.64	9.72	9.70	6.24	6.24	6.24
10	0.05	15.73	16.0	16.00	10.16	10.20	10.16
	0.10	15.73	16.0	16.00	9.33	9.35	9.33
	0.20	15.49	15.8	15.44	8.02	8.03	8.02
15	0.05	15.73	16.0	16.00	12.36	12.4	–
	0.10	15.73	16.0	16.00	11.36	11.4	–
	0.20	15.73	16.0	16.00	9.77	9.80	–
20	0.05	15.73	16.0	–	14.52	14.6	–
	0.10	15.73	16.0	–	13.36	13.4	–
	0.20	15.73	16.0	–	11.51	11.6	–

and eccentricities is presented in Table 3. It is found that under biaxial compression, with an increase in ratio of bending stiffness or area ratio, the buckling parameter decreases for simply supported boundary condition. It is observed that there is a decrease in buckling parameter with an increase of aspect ratio.

Table 3. Buckling parameter $k = \lambda b^2/\pi^2 D$ for uniformly compressed all edges simply supported square stiffened plate with varying stiffness and eccentricities ($\nu = 0.3$).

e/t	EI_s/bD					
	2.5		5.0		10.0	
	Present	[14]	Present	[14]	Present	[14]
0.0	7.908	7.930	11.7708	11.72	15.03	16
1.25	7.713	7.756	11.5399	11.54	15.03	16
2.50	7.581	7.234	11.4384	11.08	15.03	16
4.00	7.054	7.003	11.1566	10.11	15.03	16

3.3. Buckling of rectangular stiffened plates with different boundary conditions

Rectangular stiffened plates with a concentric central stiffener were analyzed for two aspect ratios of the plate and for different proportions and rigidities of the stiffener, and the buckling parameters are presented in Table 4. As before, the ratio of the cross-sectional area of the stiffener to that of the plate (A_s/bt) varied from 0.05 to 0.20 and the ratio of the bending stiffness of the stiffener to that of the plate (EI_s/bD) varied from 5 to 20. The torsional inertia of the stiffener was neglected in the analysis. These results are presented for the first time. It is found that under uniaxial compression, with an increase in ratio of bending stiffness or area ratio, the buckling parameter is constant with an increase of aspect ratio.

Table 4. Buckling parameter $k = \lambda b^2/\pi^2 D$ for square plate with a central concentric stiffener subjected to uniaxial and uniform compression in the stiffener direction ($\nu = 0.3$).

EI_s/bD	(A_s/bt)	Boundary Condition			
		CSCS		SCSC	
		1	2	1	2
5	0.05	18.98	13.54	21.77	18.03
	0.10	18.98	12.61	21.40	16.41
	0.20	18.98	11.03	16.47	13.85
10	0.05	18.98	16.64	21.76	21.18
	0.10	18.98	16.64	21.76	21.25
	0.20	18.98	16.66	21.76	19.63
15	0.05	18.98	16.66	21.76	21.17
	0.10	18.98	16.66	21.76	21.16
	0.20	18.98	16.66	21.76	21.26
20	0.05	18.98	16.66	21.76	21.15
	0.10	18.98	16.66	21.76	21.15
	0.20	18.98	16.66	21.76	21.22

3.4. Buckling of skew stiffened plates with different boundary conditions

Skew stiffened plates with a concentric central stiffener shown in Fig. 7, and having different boundary conditions were analyzed for different skew angles and the buckling parameters are presented in Table 5. The present results agree well with the finite element results of [14] and those of [12] who analyzed the problem using B-spline functions. It is observed that with an increase in skew angle, the buckling parameter increases.

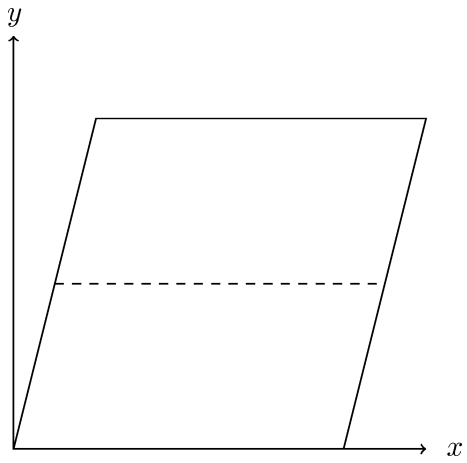

Fig. 7. Skew stiffened plate.

Table 5. Buckling parameter $k = \lambda b^2/\pi^2 D$ for skew stiffened plate (Aspect Ratio = 1.0, $EI_s/bD = 10.0$, $GJ_s/bD = 0.0$, $A_s/bt = 0.1$, $\nu = 0.3$).

Boundary condition	Skew angle	Present	[12]	[14]
All edges simply supported	0	16.00	16.00	16.00
	30	19.96	20.28	20.90
	45	27.68	28.68	29.89
All edges clamped	0	24.24	24.89	30.8
	30	32.41	33.74	36.9
	45	47.97	51.62	56.3

3.5. Buckling of uniformly compressed diametrically stiffened circular plates

The buckling loads for all the edges simply supported (SS) and clamped (CC) circular plates with concentric stiffeners along the diameters shown in Figs. 8 and 9 are computed with varying flexural and torsional stiffness parameters of the stiffener and the results are presented in the form of buckling parameter $k = (N_r)_{cr} a^2/D$ where $(N_r)_{cr}$ is the critical compressive force uniformly distributed around the edge of the plate, a is the radius of the circular plate and D is the flexural rigidity of the plate. The results are presented in Table 6. These results are presented for the first time. It is observed that with an increase in the ratio of bending stiffness, the buckling parameter increases. It is found that there is a slight increase in the buckling parameter with an increase in torsional stiffness ratio.

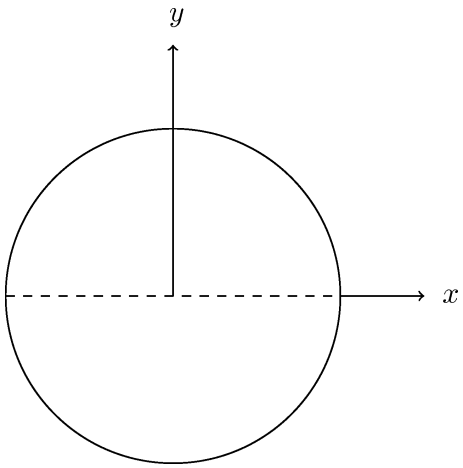

Fig. 8. Single stiffened circular plate.

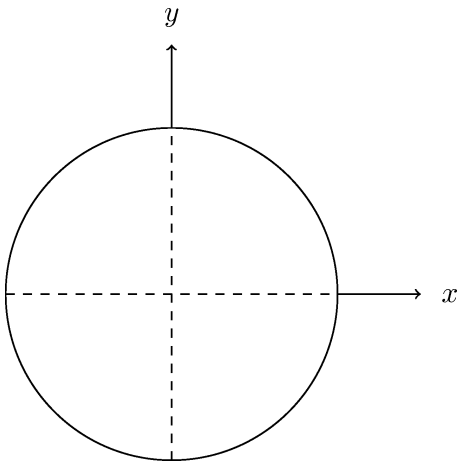

Fig. 9. Cross-stiffened circular plate.

Table 6. Buckling parameter $k = (N_r)_{cr}a^2/D$ for uniformly compressed circular plates with concentric stiffeners along the diameter with varying flexural and torsional stiffness parameters of the stiffener ($A_s/at = 0.1$, $\nu = 0.3$).

$\frac{EI_s}{aD}$	$\frac{GJ_s}{aD}$	k					
		Single stiffener		Cross stiffeners		Unstiffened	
		SS	CC	SS	CC	SS	CC
5	0.0	4.20	14.72	4.20	14.72	4.20	14.71
	2.5	7.09	26.64	10.79	44.34		
	5.0	9.66	26.65	16.67	44.35		
	7.5	11.92	26.65	22.21	44.35		
	10	13.19	26.65	27.22	44.35		
15	0.0	4.20	14.72	4.20	14.72		
	2.5	4.27	14.97	4.63	16.28		
	5.0	4.27	14.97	4.63	16.29		

4. Conclusions

Despite the huge wealth of plate elements available in literature, there is hardly a common successful element to address the problem relating to thin plates having arbitrary plate geometries. This has prompted the present investigation to propose elements for different kinds of analysis of plates. In this paper, stability analysis of stiffened plates of various configurations was carried out using a new stiffened-plate bending element. The element has the efficiency of an isoparametric element, in that a single conventional rectangular element is capable of accommodating arbitrary shapes of plates having straight, skew or curved boundaries. The formulation for the stiffener element is generalized in such a manner that the stiffener can be placed anywhere on the plate with any orientation or disposition. The results obtained in the analysis were compared with the published ones and found to agree well. Also, some new results have been presented. It was found that with an increase in bending stiffness, the buckling parameter increases for uniform cross section while it decreases more for the aspect ratio.

References

[1] A. Adini, R.W. Clough. Analysis of Plate Bending by the Finite Element Method. Report submitted to the National Science Foundation. G7337, 1961.

[2] R.J. Melosh. Basis for derivation of matrices for the direct stiffness method. *AIAA Journal*, **1**: 1631–7, 1963.

[3] M. Barik, M. Mukhopadhyay. Free flexural vibration analysis of arbitrary plates with arbitrary stiffeners. *Journal of Vibration and Control*, **5**: 667–683, 1999.

[4] M. Barik, M. Mukhopadhyay. Finite element free flexural vibration analysis of arbitrary plates. *Finite Elements in Analysis and Design*, **29**: 137–151, 1998.

[5] M. Barik. Finite element static, dynamic and stability analyses of arbitrary stiffened plates. Ph.D. Thesis, Ocean Engineering and Naval Architecture Department, Indian Institute of Technology, Kharagpur, 1999.

[6] O.K. Bedair. A contribution to the stability of stiffened plates under uniform compression. *Computers & Structures*, **66**(5): 535–570, 1998.

[7] C.J. Brown, A.L. Yettram. The elastic stability of stiffened plates using the conjugate load/displacement method. *Computers & Structures*, **23**(3): 385–391, 1986.

[8] B.H. Coburn, Z. Wu, P.M. Weaver. Buckling analysis of stiffened variable angle tow panels. *Composite Structures*, **111**: 259–270, 2014.

[9] P.E. Fenner, A. Watson. Finite element buckling analysis of stiffened plates with filleted junctions. *Thin-Walled Structures*, **59**: 171–180, 2012.

[10] M.W. Guo, I.E. Harik, W.X. Ren. Buckling behavior of stiffened laminated plates. *International Journal of Solids and Structures*, **39**(11): 3039–3055, 2002.

[11] C. Mittelstedt. Closed-form buckling analysis of stiffened composite plates and identification of minimum stiffener requirements. *International Journal of Engineering Science*, **46**(10): 1011–1034, 2008.

[12] T. Mizusawa, T. Kajita, M. Naruoka. Buckling of skew plate structures using B-spline functions. *International Journal for Numerical Methods in Engineering*, **15**(1): 87–96, 1980.

[13] M. Mukhopadhyay. Vibration and stability analysis of stiffened plates by semi-analytic finite difference method, part I: consideration of bending displacements only. *Journal of Sound and Vibration*, **130**(1): 27–39, 1989.

[14] M. Mukhopadhyay, A. Mukherjee. Finite element buckling analysis of stiffened plates. *Computers & Structures*, **34**(6): 795–803, 1990.

[15] S. Panda, M. Barik. Finite element buckling analysis of thin plates with complicated geometry. International Congress and Exhibition "Sustainable Civil Infrastructures: Innovative Infrastructure Geotechnology", 867–871, 2016.

[16] S.N. Patel, A.H. Sheikh. Buckling response of laminated composite stiffened plates subjected to partial in-plane edge loading. *International Journal for Computational Methods in Engineering Science and Mechanics*, **17**(5–6): 322–338, 2016.

[17] L.X. Peng, S. Kitipornchai, K.M. Liew. Analysis of rectangular stiffened plates under uniform lateral load based on FSDT and element-free Galerkin method. *International Journal of Mechanical Sciences*, **47**(2): 251–276, 2005.

[18] L.X. Peng, K.M. Liew, S. Kitipornchai. Buckling and free vibration analyses of stiffened plates using the FSDT mesh-free method. *Journal of Sound and Vibration*, **289**(3): 421–449, 2006.

[19] S. Peng-Cheng, H. Dade, W. Zongmu. Static, vibration and stability analysis of stiffened plates using B-spline functions. *Computers & Structures*, **27**(1): 73–78, 1987.

[20] K. Ramkumar, H. Kang. Finite element based investigation of buckling and vibration behaviour of thin walled box beams. *Applied and Computational Mechanics*, **7**: 155–182, 2013.
[21] R. Rikards, A. Chate, O. Ozolinsh. Analysis for buckling and vibrations of composite stiffened shells and plates. *Composite Structures*, **51**(4): 361–370, 2001.
[22] P. Shi, R.K. Kapania, C.Y. Dong. Vibration and buckling analysis of curvilinearly stiffened plates using finite element method. *AIAA Journal*, **53**(5): 1319–1335, 2015.
[23] S.K. Singh, A. Chakrabarti. Buckling analysis of laminated composite plates using an efficient C0 FE model. *Latin American Journal of Solids and Structures*, **9**(3): 1–13, 2012.
[24] A.K.L. Srivastava, P.K. Datta, A.H. Sheikh. Buckling and vibration of stiffened plates subjected to partial edge loading. *International Journal of Mechanical Sciences*, **45**(1): 73–93, 2003.
[25] A.K.L. Srivastava, P.K. Datta, A.H. Sheikh. Dynamic instability of stiffened plates subjected to non-uniform harmonic in-plane edge loading. *Journal of Sound and Vibration*, **262**(5): 1171–1189, 2003.
[26] A.Y. Tamijani, R.K. Kapania. Buckling and static analysis of curvilinearly stiffened plates using mesh-free method. *AIAA Journal*, **48**(12): 2739–2751, 2010.
[27] S.M. Timoshenko, J.M. Gere. *Theory of Elastic Stability*, 2nd Edition, McGrawHill International, New York, 1961.
[28] O.C. Zienkiewicz, R.L. Taylor. *The Finite Element Method*, 4th Edition, McGraw-Hill, 1989.